Journal of Applied Polymer Science

Understanding the foamability and mechanical properties of foamed polypropylene blends by using extensional rheology

Ester Laguna-Gutierrez,[1] Rob Van Hooghten,[2] Paula Moldenaers,[2] Miguel Angel Rodriguez-Perez[1]
[1]Cellular Materials Laboratory (CellMat), Condensed Matter Physics Department, University of Valladolid, 47011 Valladolid, Spain
[2]Department of Chemical Engineering, KU Leuven, B 3001 Heverlee Leuven, Belgium
Correspondence to: E. Laguna-Gutierrez (E-mail: ester.laguna@fmc.uva.es)

ABSTRACT: In this article, the influence of the rheological behavior of miscible blends of a linear and a high melt strength, branched, polypropylene (HMS PP), on the cellular structure and mechanical properties of cellular materials, with a fixed relative density, has been investigated. The rheological properties of the PP melts were investigated in steady and oscillatory shear flow and in uniaxial elongation in order to calculate the strain hardening coefficient. While the linear PP does not exhibit strain hardening, the blends of the linear and the HMS PP show pronounced strain hardening, increasing with the concentration of HMS PP. Related to the cellular structure, in general, the amount of open cells, the cell size, and the width of the cell size distribution increase with the amount of linear PP in the blends. Also mechanical properties are conditioned by the extensional rheological behavior of PP blends. Cellular materials with the best mechanical properties are those that have been fabricated using large amounts of HMS PP. The results demonstrate the importance of the extensional rheological behavior of the base polymers for a better understanding and steering of the cellular structure and properties of the cellular materials. © 2015 Wiley Periodicals, Inc. J. Appl. Polym. Sci. **2015**, *132*, 42430.

KEYWORDS: blends; foams; mechanical properties; rheology; structure–property relationship

Received 2 January 2015; accepted 29 April 2015
DOI: 10.1002/app.42430

INTRODUCTION

A polymeric cellular material consists of a two-phase structure, in which a gaseous phase, derived from a blowing agent, has been dispersed in a solid polymeric matrix.[1,2] This structure allows these materials to be used in applications such as packaging, sports and leisure, toys, thermal insulation, automotive, military, aircraft, buoyancy, or cushioning.[3] Particularly, polyolefin-based cellular materials keep some of the properties of polyolefins such as toughness, flexibility, resistance to chemicals and abrasion, and recyclability.[4,5] Currently, polyethylene (PE)-based cellular materials dominate the market of polyolefin foams. However, owing to the favorable properties of polypropylene (PP), its use has been considered in the industry, even replacing PE foams or other rigid foams such as polystyrene or polyurethane. PP is superior to PE in several aspects. It has a high melting temperature, stiffness, and the capability of static load bearing. Moreover, PP has a cost similar to PE, good temperature stability, and a good chemical resistance.[6]

Nevertheless, foaming of common linear PP is not a simple task, owing to its rheological properties, especially owing to its weak melt strength.[7,8] It is difficult to achieve high expansion ratios (ERs) during foaming because the cell walls break and the foam is not able to retain the gas during the expansion process.[9] A way to improve the foaming of a linear PP is to incorporate long-chain branches (LCBs).[10] The PPs with LCBs have a pronounced strain hardening, which is closely related to an enhancement of the melt strength.[11] Different methods have been applied to modify PP by LCB. Most of the LCB PPs are produced by *in situ* polymerization and by post-reactor treatment. After the reactor treatment, the LCBs can be formed by reactive extrusion or by electron beam irradiation.[12,13] Nowadays, several LCB PP commercial grades are available.

Several studies have shown that foaming of LCB PPs, either pure branched PP or blended with linear PP, leads to higher ERs and more homogeneous cellular structures.[9,14–16] Naguib *et al.*[9] analyzed the way to obtain larger volume ERs. For this purpose, they used a branched PP and long-chain blowing agents (pentane and butane). The fabrication route used was extrusion foaming. They also lowered the melt temperature and optimized the process conditions. The ER obtained from the linear PP was much lower than that from the branched PP, which indicates that branched PPs are more effective for the production of low-density foams. Park and Cheung[15] studied the cell nucleation and initial growth in linear and branched PP-based cellular materials foamed by extrusion. While the degree of cell coalescence was severe in the linear PP foams and

most of the cells were interconnected to each other, the branched PP gave a better foam structure. Nam *et al.*[16] studied the effect of modifying PP by the addition of LCB and the resulting effects on the rheological properties and performance of extrusion foams. More specifically, when PPs had LCBs, the foam density became lower. It was determined that the long-chain branching of PP was the main factor affecting the foam density.

The effect of blending linear and LCB PPs on foam properties has been the subject of different studies.[17–19] Reichelt *et al.*[17] described the optimization of the physical foaming by extrusion, changing different parameters, of a LCB PP and the corresponding blends with a PP block copolymer. They found a correlation between the extensional rheology and the lower limit of foam density for the blends. Blends rich in LCB PP show better foamability owing to their higher melt strength. Spitael and Macosko[18] investigated the influence of the strain hardening on foaming by extrusion of blends of linear and LCB PPs. They did not find a direct correlation between the amount of strain hardening and the foam cell density. The balance between the large nucleation of the linear PP and the reduction of the cell coalescence due to the important strain hardening of the LCB PP can lead to a higher cell concentration in the blends of linear and branched PPs than in the neat polymers. Stange and Münstedt[19] studied the influence of LCBs on the foaming behavior of PP. Different branching contents were achieved by blending a linear PP and a LCB PP. They found an almost linear increase of the strain hardening with the amount of LCB PP. Moreover, in the foaming tests, they observed a significant increase of the ER (reduction of density) by the addition of LCB PP, although this value remained constant from a concentration of the LCB PP higher than 50%. Related with the average cell size, they found that cell size decreased with the amount of LCB PP, which can be explained by a reduction of cell coalescence and cell collapse due to the increased melt strength.

Because of the foaming method used in these papers (extrusion foaming) foam density was not constant for materials containing different amounts of LCBs. These different densities make it difficult to compare between the different foams and to analyze the structure–property relationships. Moreover, the characterization of the cellular structure was mainly based on the average cell size and cell density. A more detailed characterization of the structure was typically not reported. Finally, the size and shape of the produced materials were not sufficient to measure mechanical properties in compression tests.

Bearing these limitations in mind, one of the aims of this study is to investigate the effect of long-chain branching on the cellular structure and mechanical properties of PP-based cellular materials with the same density. For this purpose, different branching contents were achieved by blending a linear and a HMS PP. Cellular materials were fabricated by improved compression molding (ICM), a technique that allows controlling the foam density. A detailed characterization of the cellular structure has also been carried out. In addition, this investigation aims to analyze the importance of the rheological behavior in the foaming process and to find a relationship between the strain hardening, the cellular structure, and the mechanical properties of PP-based cellular materials.

EXPERIMENTAL

Materials

Two different PPs have been used. The first PP is a branched high melt strength PP (HMS PP) supplied by Borealis (PP Daploy WB 135 HMS) with a tensile modulus of 2000 MPa. The second PP is a linear PP (linear PP) supplied by Total Petrochemicals (PPH 4070) with a tensile modulus of 1950 MPa. The density at room temperature is 900 kg m^{-3} for both PPs.

Blends of the two PPs at different contents of linear PP (10, 25, 50, 75, and 90 wt %) have been prepared with a co-rotating twin screw extruder Collin ZK 25T with L/D of 24. The rotational speed used was 80 rpm and the melt temperature was 190°C. The sample code used with the different blends is the following: wt % HMS PP – wt % linear PP.

Antioxidants Irgafos 168 and Irganox 1010 (from Ciba) have also been used to reduce the thermal degradation of the polymers.

The foaming was performed using a chemical blowing agent, azodicarbonamide (ADC) Lanxess Porofor M-C1 with an average particle size of 3.9 ± 0.6 μm and a decomposition temperature of 210°C.

Foaming Process

ICM is a technique that allows controlling, regardless of the formulation, the density of cellular materials. In addition, the volumes produced by this technique are large enough to subsequently perform compression tests or other macroscopic characterizations.[20–22]

Before the foaming process, the pellets containing the blowing agent were fabricated. For this purpose, the formulations produced were mixed with 3 wt % of ADC using the same co-rotating twin screw extruder, previously described, with a rotational speed of 100 rpm and a melt temperature of 180°C. Irgafos 168 in a proportion of 0.08% and Irganox 1010 in a proportion of 0.02% by weight were added to the formulation.

Once the final formulation was fabricated, the pellets are placed in a mold [Figure 1(a)], which is located in a hot-plate press. An initial pressure (P_0) is applied to the system while it is heated until the foaming temperature (T_F), which is higher than the decomposition temperature of the blowing agent [Figure 1(b)]. As the temperature increases, the blowing agent starts decomposing and the pressure inside the mold increases up to a value (P_F). After a certain time (t_F), when the blowing agent is fully decomposed, and P_F does not continue to increase, the pressure of the press is released allowing the polymer to expand until the desired ratio [Figure 1(c)]. A scheme of the mold and of the ICM technique is shown in Figure 1.

Finally, the mold is introduced in cold water to cool down the sample and hence stabilizing the cellular structure as fast as possible.[23]

Foaming parameters t_F, P_0, and T_F can be chosen depending on the polymeric matrix type, chemical composition, blowing agent

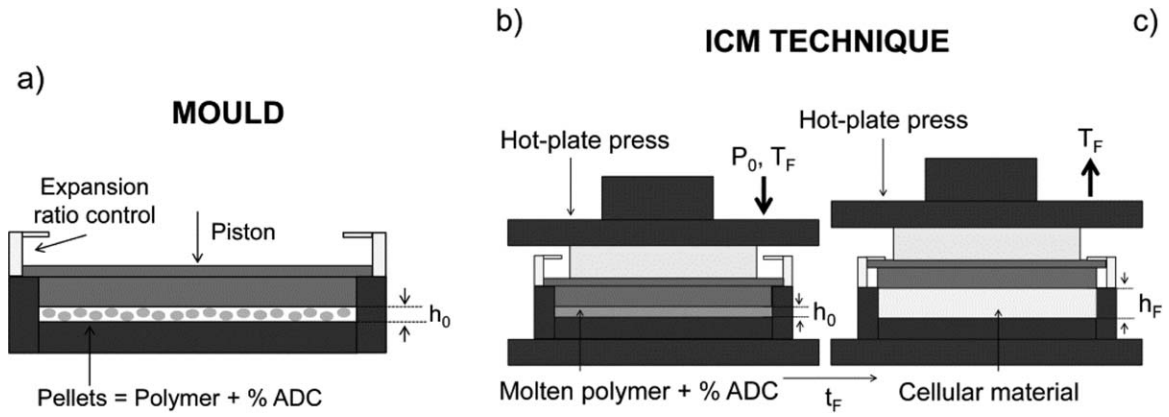

Figure 1. (a) Scheme of the mold used in the ICM technique. (b) Heating of the system until the foaming temperature (T_F) under a pressure P_0. (c) Release of pressure allowing the polymer to expand from an initial height (h_0) to a final height (h_f).

concentration, and sample geometry. In this case, t_F was 15 min, P_0 was 41.5 bars, and T_F was 200°C. These parameters were maintained for all the cellular materials fabricated.

The control of foam density is essential in this study. It is carried out by means of a self-expandable mold as can be seen in Figure 1. Owing to this, density can be fixed at a given value.[20–22] All the cellular materials have been fabricated with a density of 180 kg m^{-3} (ER 5 and relative density 0.2) independently on the chemical composition used. Foamed samples were discs with 150 mm in diameter and 10 mm in thickness.

Samples Characterization

Differential Scanning Calorimetry. Thermal properties of the pure PPs and the different PP blends were studied by means of a Mettler DSC822e differential scanning calorimeter, previously calibrated with indium, zinc, and *n*-octane. The weight of the samples was ~5.5 mg.

The melt and crystallization temperature were determined according to the following thermal protocol:

- First segment: Samples were heated from −40 to 250°C at a heating rate of 10°C min^{-1} under nitrogen atmosphere. In order to remove materials thermal history, an isothermal segment (3 min) was added at the end of this heating segment.
- Second segment: Samples were cooled from 250 to −40°C at a cooling rate of 10°C min^{-1} under nitrogen atmosphere.
- Third segment: Samples were heated a second time from −40 to 250°C at a heating rate of 10°C min^{-1} also under nitrogen atmosphere.

The melt temperature (T_m) was taken at the minimum of the heat flow–temperature curve (third segment). The crystallization temperature (T_c) was taken at the maximum of the heat flow–temperature curve (second segment), and also the difference between the melt temperature and the crystallization temperature ($\Delta T = T_m - T_c$) was calculated.

Rheological Behavior. Shear rheological measurements were performed at a temperature of 200°C under nitrogen atmosphere using a parallel plates geometry of 25 mm in diameter and a gap of 1 mm. Cylindrical samples (without blowing agent) with a thickness of 1.5 mm and a diameter of 22 mm were prepared in a hot plate press at a temperature of 220°C. A stress-controlled rheometer AR 2000 EX from TA Instruments was used to perform the tests.

Dynamic-mechanical experiments over an angular frequency range of $0.1 < \omega < 100$ rad s^{-1} were performed for all materials. A strain of 5% was used, which was in the linear viscoelastic regime for all samples. In this frequency range, the response regime, where G'' and G' and are proportional to ω and ω^2, respectively, was not reached. This regime was achieved by the application of time–temperature superposition, after performing measurements at a temperature of 250°C. Only the blends 100–0, 50–50, and 0–100 have been measured at 250°C. In addition to the oscillatory experiments, the start-up and steady-state shear viscosity were measured at different shear rates (between 0.004 and 1 s^{-1}).

Extensional rheology of the neat PPs and the different blends was measured using a strain-controlled rheometer (Ares-2K from TA Instruments) with the extensional viscosity fixture (EVF). In this geometry, two cylinders are used to wind-up the sample. One cylinder is rotating and the other measuring the force. In order to wind-up the sample equally on both sides, the rotating cylinder moves on a circular orbit around the force-measuring cylinder while rotating around its own axis at the same time. All the experiments were made at a temperature of 200°C (this is the same temperature at which the foaming process was performed). Rectangular solid samples, with dimensions of 20 mm × 10 mm × 0.5 mm ($L \times W \times T$), fabricated by compression molding, at a temperature of 200°C and a pressure of 21.8 bars, were used.

The following measurement protocol was applied:

- Pre-stretch: Once the sample is attached to the drums and it has melted a pre-stretch is performed in order to compensate the thermal expansion of the sample when it is heated up from room temperature. This pre-stretch was done at a Hencky strain rate of 7.5×10^{-3} s^{-1}.
- Relaxation post pre-stretch: When the pre-stretch is finished, the sample is kept for 30 s at a constant temperature (200°C) without applying any stress.

- Test: After this relaxation the experiment takes place. The measurements have been performed at three different Hencky strain rates: 0.1, 0.3, and 1 s^{-1}. The final Hencky strain has been 3 for all the different materials.

To evaluate the extensional viscosity measurements it is necessary to know the density at the temperature at which the experiment is being performed. For PPs this melt density is tabulated.[24] The melt density at a temperature of 200°C for PP is 750 kg m^{-3}.

Mechanical Tests. For the cellular materials, mechanical properties in compression have been measured. Stress (σ)–strain (ε) curves were obtained with an Instron Machine (model 5.500R6025) at room temperature and at a strain rate of 10 mm min^{-1}. The maximum static strain was 75% for all the experiments. The compression experiments were performed according to the standard ASTM D1621. Samples were cubes with dimensions of 20 mm × 20 mm × 10 mm ($L \times W \times T$) cut from the samples produced by ICM. The compression tests have been performed on two different samples of the same cellular material and always in a parallel direction to the foaming direction (thickness direction). Three mechanical properties were obtained from these experiments: elastic modulus (E), collapse stress (σ_C), which was measured in the intersection between a parallel line to the stress–strain response at low strains and a parallel line to the plateau region of the stress–strain curve, and absorbed energy per unit volume (W) that has been calculated as the area under the stress–strain curve up to 75% strain.

Density. Density of the cellular materials was determined by using the geometric method: dividing the weight of each specimen by its corresponding volume (ASTM standard D1622-08). Density was measured for 10 different samples from the cellular material. These samples were cubes with dimensions of 20 mm × 20 mm × 10 mm ($L \times W \times T$).

Open Cell Content. Open cell content of foamed materials was determined according to the ASTM Standard D6226-10 using a gas pycnometer Accupyc II 1340 from Micromeritics.

The following equation was used according to the ASTM standard:

$$\mathrm{OC}(\%) = 100\left(\frac{V_{\mathrm{sample}} - V_{\mathrm{pyc}}}{V_{\mathrm{sample}} \cdot p}\right), \tag{1}$$

where V_{sample} is the geometrical volume of the sample, V_{pyc} is the volume measured by the gas pycnometer, p is the sample porosity calculated by $\left(1-\frac{\rho_{cm}}{\rho_s}\right)$, ρ_{cm} is the cellular material density, and ρ_s is the solid matrix density.

If the open cell content of the samples is 0% (the material has closed cells) the volume measured by the pycnometer matches the geometrical volume because the gas is not able to penetrate the foam. However, if the samples have a 100% of open cell content the volume measured by the pycnometer is only the volume of the solid phase in the cellular material, distributed between the struts and walls, because the gas in this case is able to penetrate the foam throughout the interconnections between cells.

Structural Characterization. Scanning electron microscopy (SEM) was used to analyze the cellular structure, and also to quantify the cell size distribution, the average cell size (Φ), the anisotropy ratio (AR), the standard deviation coefficient of the cell size distribution relative to the cell size (SDC/Φ), the cell density (N_V), and the coalescence ratio (CR). For this purpose, the micrographs obtained were analyzed with an image processing tool based on the software Image J.[25]

Samples were cooled using liquid nitrogen to cut them without modifying their structure; then, they were vacuum coated with a thin layer of gold to make them conductive. A Jeol JSM-820 scanning electron microscope was used to observe the samples morphology. A more detailed description of the experimental techniques can be found elsewhere.[26–28]

The average cell size (Φ) for a given material is defined as indicated in eq. (2).

$$\Phi = \sum_{i=1}^{n}\frac{\Phi^i}{n} = \sum_{i=1}^{n}\frac{\mathrm{cf}}{2n}\left(\Phi_x^i + \Phi_y^i\right), \tag{2}$$

where n is the number of counted cells, Φ^i is the three-dimensional cell size of the cell i, Φ_x^i and Φ_y^i are the chord lengths of the cell i in the x and y directions, and cf is a correction factor needed to calculate the cell size in 3D from a two-dimensional value. While the average two-dimensional cell size $\left(\frac{\Phi_x^i+\Phi_y^i}{2}\right)$ is directly measured by the software, previously mentioned, a correction factor (cf) is used to calculate the three-dimensional cell size. This correction factor was determined by Pinto *et al.*[25] Moreover, in this work, the expansion direction is the y direction. The characterization has been performed only in a plane (x–y). This is because as a consequence of the foaming process employed (ICM) it holds that ($\Phi_x^i \approx \Phi_z^i$).

The AR is defined as the ratio of the chord length in the expansion direction (Φ_y^i) to that in a perpendicular direction (Φ_x^i).[29] Taking into account this definition an isotropic cell has an AR of 1.

The SDC relative to the cell size has been calculated according to eq. (3).[21,30]

$$\frac{\mathrm{SDC}}{\Phi} = \frac{1}{\Phi}\sqrt{\sum_{i=1}^{n}\frac{\left(\Phi^i-\Phi\right)^2}{n}}. \tag{3}$$

SDC/Φ is related to the width of the cell size distribution and consequently gives information about the homogeneity of the cellular structure. A low value of SDC/Φ indicates a narrow, and therefore a homogeneous cell size distribution, where all cells have a size close to the average value.

The cell density (N_V) is the number of cells per unit volume of the solid. The following expression [eq. (4)] has been used to calculate the cell density.

$$N_V = \frac{6}{\pi\Phi^3}\left(\frac{\rho_s}{\rho_{\mathrm{cm}}} - 1\right). \tag{4}$$

In the case of no coalescence N_V measures the cell nucleation density.[25]

Table I. DSC Results of the Polypropylene Blends

Sample (HMS PP–linear PP)	T_m (°C)	T_c (°C)	ΔT (°C)
100–0	161.5	127.3	34.2
90–10	162.2	126.7	35.5
75–25	162.7	126.8	35.9
50–50	163.7	126.5	37.2
25–75	165.2	126.0	39.2
10–90	165.9	125.1	40.8
0–100	164.3	121.4	42.9

Finally, the CR has been calculated as the ratio between the potential nucleation density and the measured cell density (N_V).

$$\mathrm{CR} = \frac{\mathrm{Nucleants/cm^3}}{N_V}. \tag{5}$$

Chemical blowing agents such as ADC are self-nucleating particles for the cells, which means that when the blowing agent content increases, a greater number of nucleating sites are available.[2,22] The potential nucleation density can be calculated according to eq. (6).

$$\frac{\mathrm{Nucleants}}{\mathrm{cm^3}} = \frac{W_P \rho_C}{\rho_P V_P}, \tag{6}$$

where W_P is the weight fraction of the ADC particles used to produce the cellular materials, ρ_C is the density of the polymeric composite (PP + ADC), ρ_P is the density of particles, the ADC particles, and V_P is the volume of an individual particle. In this case it has been assumed that ADC particles are 3.9 μm side cubes. The ADC density is 1600 kg m^{-3}.

RESULTS AND DISCUSSION

Thermal Characterization

Table I shows the melting point (T_m), the crystallization temperature (T_c), and the difference between the melt temperature and the crystallization temperature (ΔT) for the different materials, obtained from the differential scanning calorimetry (DSC) curves. This difference is very important to analyze the stabilization of the cellular structure. The smaller the difference is, the quicker the stabilization of the cellular structure occurs, i.e., the cellular structure has less time to degenerate during the cooling process.

The difference between both temperatures increases significantly (nearly 9°C) if the content of linear PP increases. Therefore, from the point of view of the DSC results, it is more favorable to work with the HMS PP than with the linear PP in order to stabilize as fast as possible the cellular structure.

Rheological Behavior

The modulus of the complex shear viscosity (η^*) of the linear PP, the HMS PP, and the blend 50–50 is shown in Figure 2.

The dynamic shear viscosity of the HMS PP is somewhat lower than that of the linear PP. Blend 50–50 has a value of the viscosity between the values of the linear PP and the HMS PP. The difference between the viscosity of the linear and the HMS PP becomes more pronounced at higher frequencies. The HMS PP is the material, which exhibits the most pronounced shear thinning behavior owing to the presence of LCBs and the significant contribution of the high molecular weight parts. In this material the transition to the Newtonian plateau region occurs at lower frequencies.[31,32] In addition, it can be observed that the Newtonian plateau has been reached for the three materials at low frequencies.

To analyze the miscibility of both PPs the logarithmic additivity rule for low-molecular-weight-based blends is used.[33] This rule is expressed as follows:

$$\log(\eta^*(\omega)) = \varphi_{\mathrm{HMS\ PP}} \log\left(\eta^*(\omega)_{\mathrm{HMS\ PP}}\right) + (1\text{-}\varphi_{\mathrm{HMS\ PP}}) \log\left(\eta^*(\omega)_{\mathrm{linear\ PP}}\right), \tag{7}$$

where $\varphi_{\mathrm{HMS\ PP}}$ is the HMS PP content in volume percent and $\eta^*(\omega)_{\mathrm{HMS\ PP}}$ and $\eta^*(\omega)_{\mathrm{LINEAR\ PP}}$ are the complex viscosities of the pure HMS PP and the pure linear PP, respectively.

Table II shows the experimentally obtained modulus of the complex shear viscosity at a frequency of 1 rad s^{-1} and the theoretical one obtained with the log additivity rule at the same frequency. It also shows the deviation of the theoretical results from the experimental results.

The maximum deviation of the theoretical value from the experimental one is only 4%, indicating that the polymeric blends obey the log additivity rule and consequently this result suggests a clear miscibility of both PPs.

The loss angle is a very sensitive indicator of the presence of LCBs in a polymer. Figure 3 shows the loss angle (δ) as a function of frequency for the materials 100–0, 50–50, and 0–100.

The linear PP demonstrates a monotonic decrease in loss angle with frequencies. The angle approaches the value of 90° at low frequencies indicating that sample is predominantly viscous. The HMS PP, however, shows an inflection in the curve with a tendency toward a plateau at high frequencies, although in this range of frequencies the plateau is not observed. Wood-Adams *et al.*[34] reported that there was a plateau in the loss angle whose magnitude and breadth depend on the degree of LCB. Finally, it

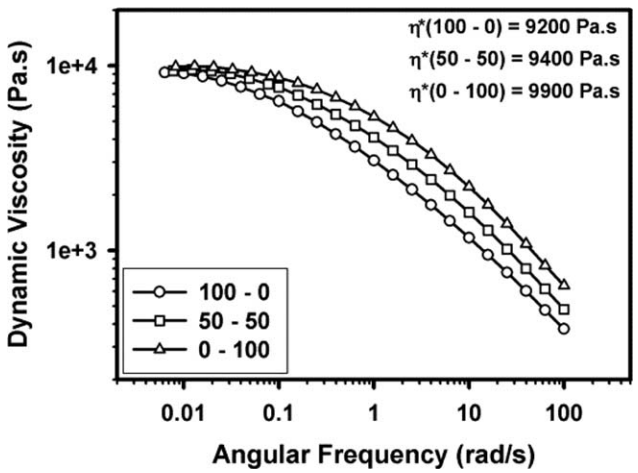

Figure 2. Dynamic shear viscosity versus angular frequency of materials: 100–0, 50–50, and 0–100.

Table II. Experimental and Theoretical Values Obtained by the Log Additivity Rule of the Complex Shear Viscosity (η^*) at a Frequency of 1 rad s^{-1} and at a Temperature of 200°C

Sample (HMS PP–linear PP)	Experimental η^* (Pa s)	Theoretical η^* (Pa s)	Deviation (%)
100-0	3065	3065	0
90-10	3198	3237	1
75-25	3420	3514	3
50-50	4088	4029	1
25-75	4792	4619	4
10-90	5050	5013	1
0-100	5295	5295	0

can be concluded that the loss angle of the HMS PP at low frequencies is somewhat lower than that of the linear PP, indicating that the HMS PP exhibits a more elastic response characteristic of solid materials.[35]

The start-up shear viscosity (η) has been measured in all the PP blends at different shear rates until the steady state was reached. Figure 4 shows the steady-state shear viscosity as a function of shear rate.

For a shear rate ($\dot{\gamma}$) of 0.01 s^{-1}, or lower, all the materials have reached a Newtonian plateau. Moreover, the shear viscosity increases with the amount of linear PP in the same way as the dynamic shear viscosity did (see Figure 2). Figure 4 also contains the values of the zero shear viscosity (η_0). Comparing the values of dynamic shear viscosity at low frequencies (at the Newtonian plateau) with the values of zero shear viscosity it can be concluded that these values are very similar and consequently these PP materials satisfy the viscoelastic limiting behavior.

$$\lim_{\omega \to 0} \eta^*(\omega) = \lim_{\dot{\gamma} \to 0} \eta\left(\dot{\gamma}\right) \tag{8}$$

Finally, extensional viscosity measurements have been performed on these PP blends. Extensional viscosity is defined as

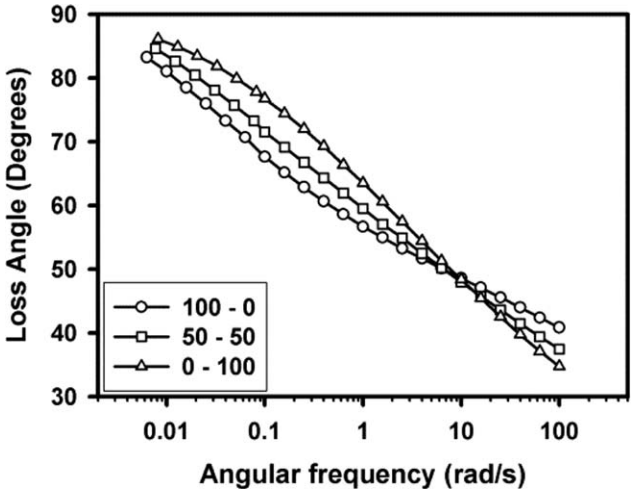

Figure 3. Loss angle versus angular frequency of materials: 100–0, 50–50, and 0–100.

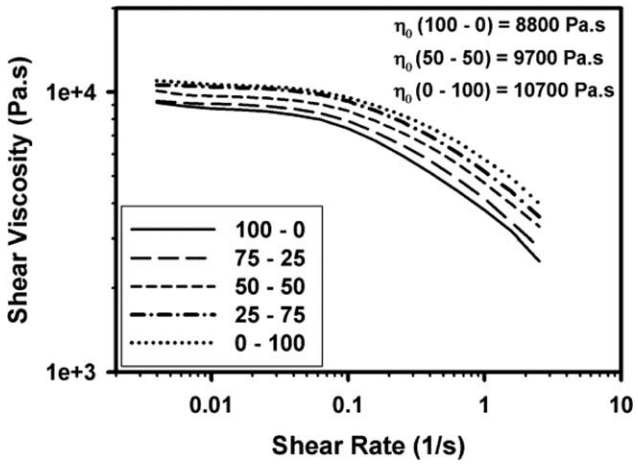

Figure 4. Shear viscosity as a function of shear rate of the pure PPs and the different blends.

the ratio between the stress and the strain rate, when a material is elongated. In some polymers, a phenomenon called strain hardening takes place, which is related to a rapid increase in extensional viscosity at high strains.[36]

The strain hardening phenomenon is associated to LCB polymers.[10,14] For polymers with the same melt flow index, an increase in the number of the long-chain branches induces strain hardening in the elongational viscosity of the melt. Because of the increase of the strain hardening behavior a strong enhancement of the melt strength appears.

Figure 5(a,b) shows the transient extensional viscosity of the seven PP blends under investigation, measured at three different Hencky strain rates. As it is indicated on the figure, the results of each blend have been multiplied by a certain value in order to compare all the materials in the same graph.

The HMS PP exhibits a pronounced strain hardening, whereas the linear PP does not display strain hardening. As the content of HMS PP increases, the slope of the curves, in the region of strain hardening, also increases.

To quantify this strain hardening behavior, the strain hardening coefficient (S), for a particular value of time and Hencky strain rate, has been determined according to eq. (9):

$$S = \frac{\eta_E^+(t, \dot{\varepsilon}_0)}{\eta_{E0}^+(t)} \quad , \tag{9}$$

where $\eta_E^+(t, \dot{\varepsilon}_0)$ is the transient extensional viscosity as a function of time and Hencky strain rate and $\eta_{E0}^+(t)$ is the transient extensional viscosity in the linear viscoelastic regime, which can be determined in two different but equivalent ways: as three times the transient shear viscosity growth curve at very low shear rates or by extrapolating the superimposed portion of the curves for different elongation rates.[37,38] In the present work, the first option has been chosen to determine S.

Figure 6 shows the strain hardening coefficient for all materials. This value has been calculated for a Hencky strain rate of 1 s^{-1} and a time of 3 s, because during the foaming process the Hencky stain rates applied are around 1 s^{-1} and the Hencky strains are approximately between 3 and 4.[18,36]

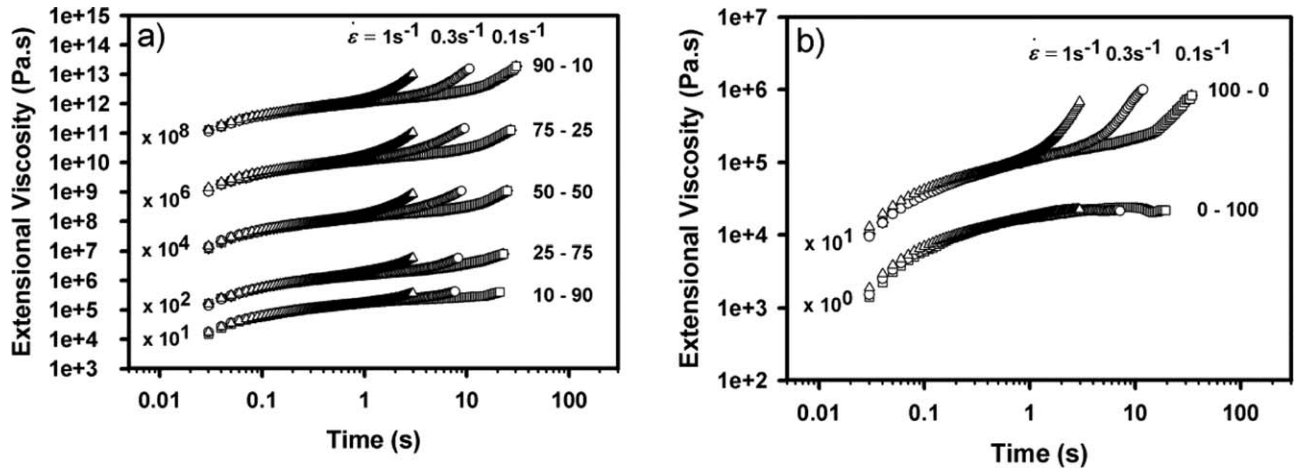

Figure 5. (a) Extensional viscosity of PP blends at different Hencky strain rates, $\dot{\varepsilon}$. (b) Extensional viscosity of pure PPs at different Hencky strain rates, $\dot{\varepsilon}$.

Essentially this coefficient increases if the amount of HMS PP increases, although this behavior is not so clear when large amounts of HMS PP are used. The linear PP has a value of S equal to 1, indicating again that this material does not present strain hardening as is also shown in Figure 5.

The shear and extensional rheological properties of the PP blends depend both on the amount of the HMS PP in the blend. However, it is clear that the extensional properties are far more sensitive to the effect of LCB. Hence, differences in the structural and mechanical properties of the resulting PP cellular materials are related to the change in the extensional properties, as the shear viscosity is only slightly decreased by the addition of the HMS PP.

Cellular Materials Density and ER

The results for the density and also for the expansion ratio (ER) of the PP cellular materials produced by the ICM route are shown in Table III. The ER is defined as the ratio between the solid density (ρ_s) and the cellular material density (ρ_{cm}).

$$\mathrm{ER} = \frac{\rho_s}{\rho_{cm}}. \tag{10}$$

The materials with contents of HMS PP higher than 25 wt % reach the expected relative density. For the other two materials the density is slightly higher and consequently the ER is slightly lower. Under the processing conditions used, these materials are not able to achieve an ER of 5. The linear polymer is not capable of supporting the induced stretching during foaming. As a result, the cell walls are broken and the gas can escape through the open cells (see next section).

Open Cell Content

The open cell content has been measured to quantify the interconnection between the cells of the different cellular materials. High open cell content leads to poor mechanical properties, low thermal insulation, good acoustic absorption, and low dimensional stability.[39–41] In thermoplastic polymers, the open cell content is related to the expansion degree. In low-density cellular materials, the polymeric matrix is subjected to high elongational forces during the foaming. Cellular walls consequently become thinner and they can easily break. For cellular materials with very similar density the extensional rheological behavior is closely related to the open cell content as it is shown in Figure 7.

When the strain hardening coefficient is low, the open cell content of the cellular material is high. For the cellular materials fabricated with a high content of HMS PP, in which S is approximately constant, the open cell content is also constant. Moreover, it can be deduced from Figure 7 that when the polymer has a value of S lower than 4, cells are completely open for the foam densities produced. As the ER and the shear rheological properties are very similar, for all blends under investigation, it can be concluded that changes in the extensional rheological behavior lead to changes in the open cell content.

The high open cell content of the pure HMS PP (about 50%) can be explained by the high content of blowing agent used to manufacture the cellular materials (3 wt %). Subsequent studies (not published) have demonstrated that the minimum amount

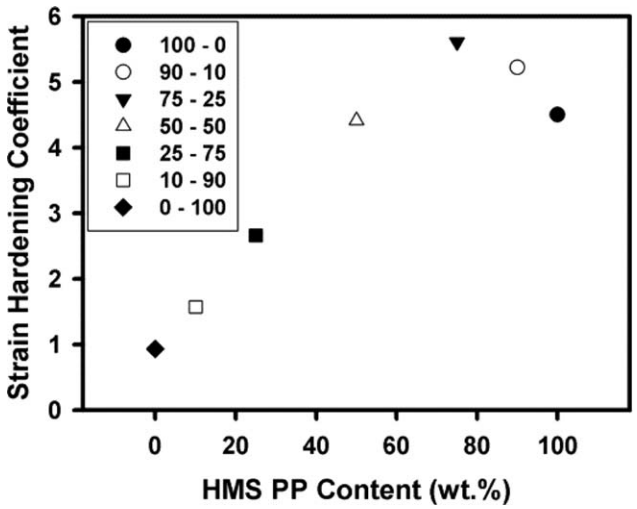

Figure 6. Strain hardening coefficient of the different blends of the HMS PP and the linear PP.

Table III. Cellular Materials Density and Expansion Ratio

Sample (HMS PP–linear PP)	Density (kg m^{-3})	SD[a] (kg m^{-3})	Expansion ratio	SD[a]
100–0	178	6	5.11	0.17
90–10	182	4	5.00	0.10
75–25	181	5	5.03	0.14
50–50	180	3	5.06	0.08
25–75	183	12	4.97	0.34
10–90	194	15	4.69	0.40
0–100	207	17	4.42	0.40

[a] Standard deviation.

of ADC required to achieve an ER of 5 with the HMS PP is almost half of that used in this study. If the amount of blowing agent is too high the open cell content can increase owing to an overpressure inside the mold during the polymer expansion process.

Cellular Structure

Figure 8 shows SEM micrographs of the different cellular materials fabricated by ICM. It is clear that the rheological properties of the blends influence the cellular structure, which in turn determines the mechanical response of PP foams.

Several conclusions can be drawn from the observation of these micrographs. First of all, SEM micrographs demonstrate, qualitatively, that the open cell content increases with the amount of linear PP, as was concluded from the quantitative pycnometry measurements (previous section). Ruptures of cell walls can be observed in the cellular materials 10–90 and 0–100. Secondly, it can be concluded that the average cell size also increases with the amount of linear PP.

Regarding the cell anisotropy, the blend 25–75 leads to a very anisotropic structure. When the amount of linear PP is reduced cells are more isotropic, although cells are never completely isotropic. The anisotropic nature of the cellular materials is mainly related to the ICM foaming process used to manufacture the cellular materials. The growth of the cellular material is restricted by the mold and the expansion can only occur in one direction, promoting this anisotropic growth.

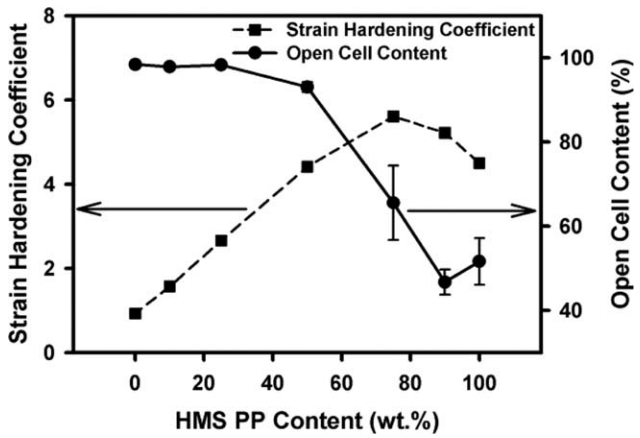

Figure 7. Correlation between the strain hardening coefficient and the open cell content.

In order to analyze the homogeneity of the cellular structure the cell size distribution of the cellular materials has been evaluated. Figure 9 shows the corresponding histograms.

All cellular materials present a wide cell size distribution. This width increases with the amount of linear PP. When the amount of HMS PP prevails the cell size distribution is narrower indicating that the cellular structure is more homogeneous. When the amount of linear PP increases the cells start to break as the polymer cannot withstand the deformation to which it is subjected and consequently larger cells begin to appear, although there are still cells that have not been broken. In fact all the histograms present a maximum for a cell size of ~250 μm; however, while the cell size of the cellular materials with a high content of HMS PP is always lower than 600 μm, in the cellular materials with a high content of linear PP there are cells with sizes up to 900 μm.

With the aim of quantifying the qualitative results previously mentioned, several characteristics of the cellular structure were measured. Figure 10 shows the results for the average cell size and AR.

The average cell size (Φ) and the AR remain almost constant for the cellular materials generated with blends with a content of the HMS PP higher than 75 wt %. In these materials also the strain hardening coefficient is almost constant. For values of the HMS PP content lower than 75 wt % and increment in the average cell size is produced when the amount of linear PP increases and therefore the strain hardening coefficient decreases. Moreover, for all these materials the open cell content is 100%, which leads to the following conclusion. PP-based open cell cellular materials with differences in the average cell size of 80 μm can be obtained by changing the proportion of linear PP and HMS PP, provided that the linear PP content is higher than 25 wt %.

Relative to the AR, the cellular material 25–75 has an AR higher than 3. This high value is a consequence of a partial rupture of the cells as well as the restricted foaming in one direction. When the amount of linear PP is higher than 75 wt % the polymer is so weak than most of the cell walls are completely broken and consequently cells lose their anisotropy.

In order to better evaluate the cell anisotropy, the average chord length in the expansion direction ($\Phi_y = \Sigma_{i=1}^{n} \frac{\Phi_y^i}{n}$) and the average chord length in a perpendicular direction to the expansion one ($\Phi_x = \Sigma_{i=1}^{n} \frac{\Phi_x^i}{n}$) have been calculated. Figure 11 shows the

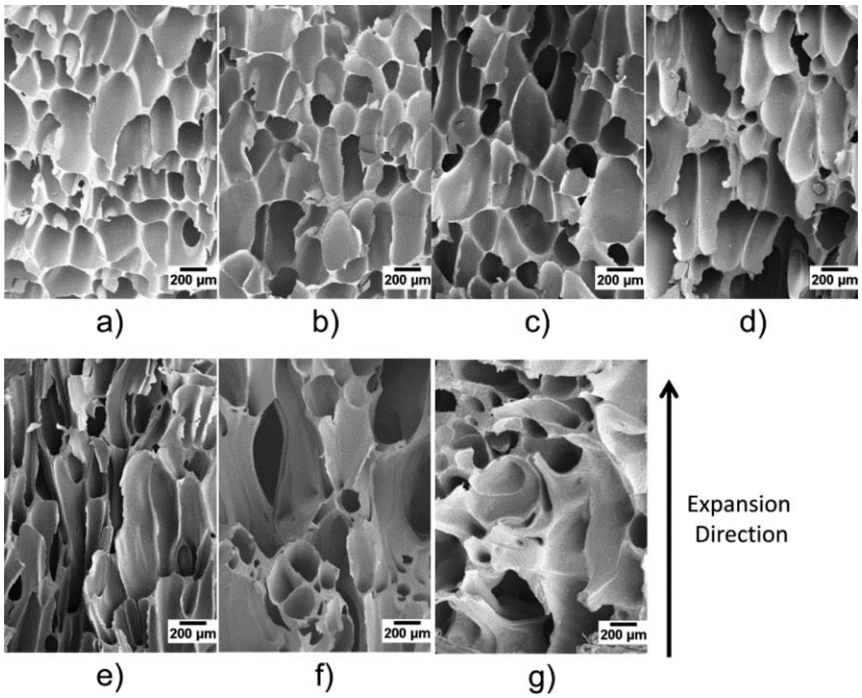

Figure 8. SEM micrographs of the cellular materials. (a) 100–0, (b) 90–10, (c) 75–25, (d) 50–50, (e) 25–75, (f) 10–90, and (g) 0–100.

average chord length in both directions as a function of the HMS PP content.

In general, the average chord length in the expansion direction (y) is higher than in the perpendicular direction (x). For cellular materials that have been fabricated with a HMS PP content higher than 75 wt % both Φ_x and Φ_y are constant. For cellular materials that have been fabricated with a HMS PP content between 25 and 75 wt %, it can be observed that while Φ_x remains almost constant Φ_Y increases with the amount of linear PP. That means that in these materials some of the cellular walls, which are perpendicular to the expansion direction, are breaking and consequently cells are growing considerably in the expansion or thickness direction, making the anisotropy to increase. Finally, when the cellular materials have been fabricated with a HMS PP content lower than 25 wt %, it can be concluded that cell coalescence is produced in both directions making the cells to growth in the expansion direction and also in the perpendicular one. As a result cell loss their anisotropy, as has been already shown in Figure 10.

Another way to analyze the cell size distribution is to use the standard deviation coefficient of the cell size distribution relative to the average cell size (SDC/Φ). Owing to the large amount of samples included in this study, the use of SDC/Φ is a good and an easy way to compare the results obtained with the different blends (Figure 12).

The highest values of SDC/Φ are obtained for the cellular materials in which the amount of linear PP is predominant, as is also shown in Figure 9. This high value means that the cellular structure is very heterogeneous presenting small and large cells with a cell size far away from the average cell size. The relationship between SDC/Φ and the open cell content is shown in Figure 13.

When the amount of linear PP increases the strain hardening decreases and consequently the materials have a higher open cell content as is shown in Figure 7. Figure 13 shows that SDC/Φ increases if the open cell content increases. As the cells are breaking, new cells appear with a larger cell size resulting in a more heterogeneous cellular structure and consequently increasing SDC/Φ. Furthermore, for cellular materials with 100% open cell, SDC/Φ continues increasing as the percentage of linear PP increases.

Another parameter, related to the cellular structure, is the cell density (N_V). Results as a function of blend composition are shown in Figure 14.

It can be observed that the number of cells per cubic centimeter increases with the amount of HMS PP. This result is consistent with the average cell size results. When the amount of HMS PP is lower than 75 wt % the cell density increases with the amount of HMS PP. For these materials the average cell size decreased with the amount of HMS PP (Figure 10) indicating, as expected, that for cellular materials with the same density the cellular density increases when the average cell size decreases. Moreover, for cellular materials with a HMS PP content higher than 75 wt % the cellular density remains almost constant in the same way than the average cell size.

Finally, to conclude this study of the cellular structure, the CR has been calculated for all materials.[22] CR has been defined in eq. (5) as the ratio between the potential nucleation density of ADC–PP mixtures and the measured cell density. CR is considered as a quantitative measurement of the

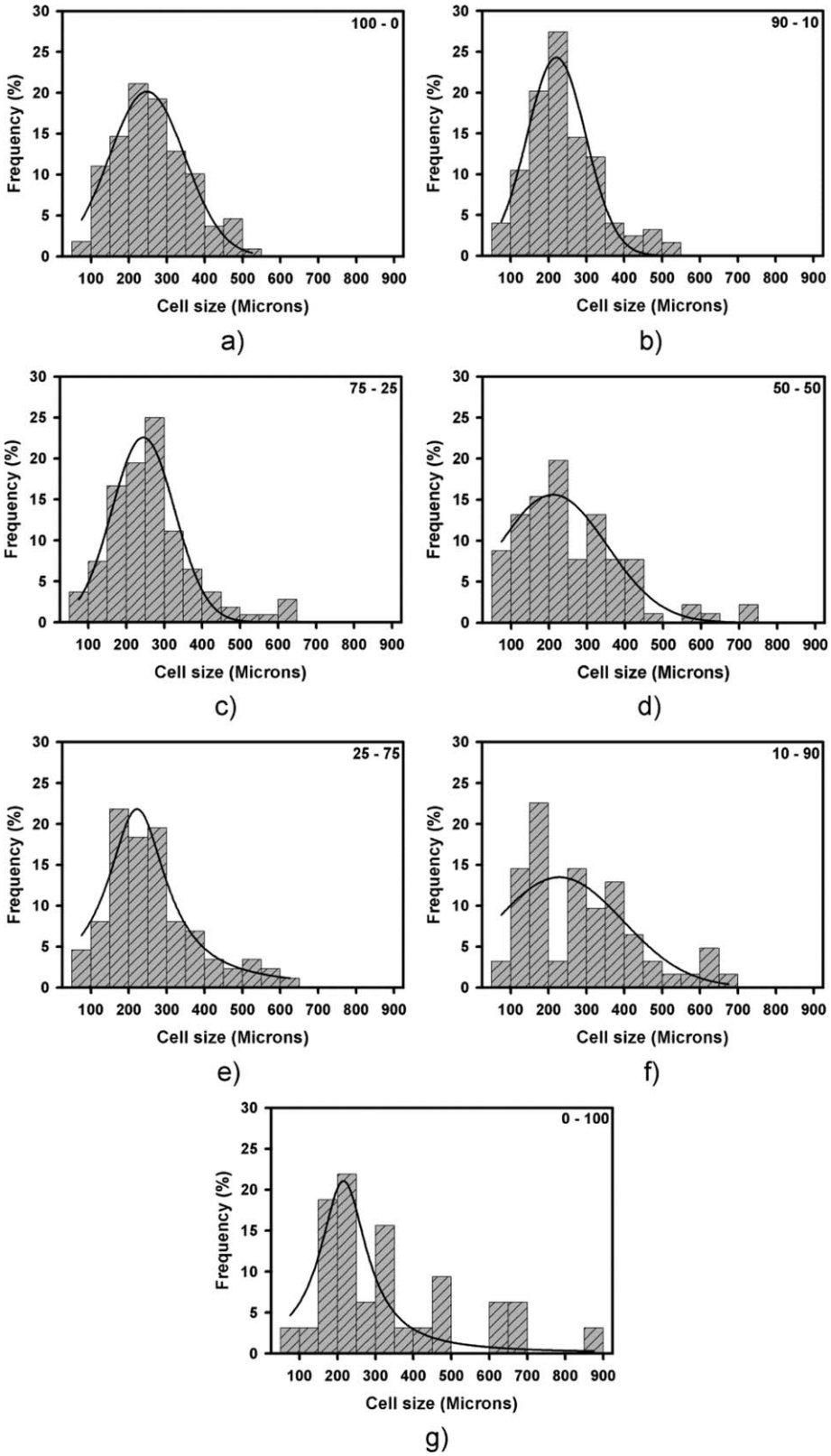

Figure 9. Cell size distribution of cellular materials. (a) 100–0, (b) 90–10, (c) 75–25, (d) 50–50, (e) 25–75, (f) 10–90, and (g) 0–100.

degeneration of the cellular structure during the foaming process. If CR is equal to 1, it means that the potential nucleation density and the cell density are the same, i.e., no degeneration of the cellular structure by coalescence or coarsening occurs. Results of CR as a function of the HMS PP content are shown in Figure 15.

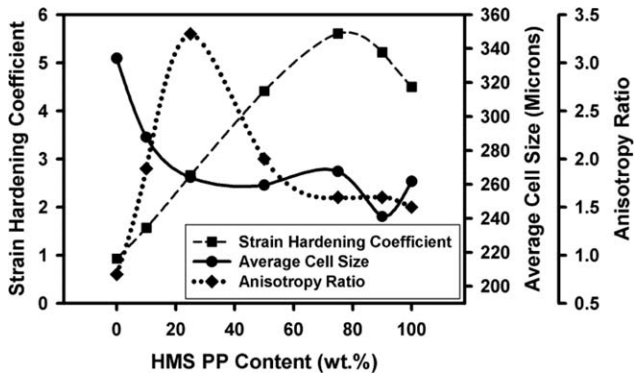

Figure 10. Effect of HMS PP content and strain hardening coefficient in the average cell size and anisotropy ratio of the cellular materials.

The CR remains constant for the cellular materials, which have been fabricated with an amount of HMS PP higher than 75 wt %. For these materials the CR is equal to 1000 which means that only 1 of every 1000 potential cells survives during the foaming process. On the other hand, when the amount of HMS PP is lower than 75 wt % the CR increases if the linear PP content also increases. For the cellular material fabricated only with the linear PP the CR is as high as 5000 indicating that in this material only 1 out of every 5000 cells survive during the foaming process. With this parameter (CR) it is easy to understand and to demonstrate how the coalescence increases if the linear PP content increases.

Mechanical Response

As with all polymer blends, the final blend properties depend on the properties of the individual components and the blend ratio. Moreover, the mechanical properties of the polymeric cellular materials also depend on the mechanical properties of the solid matrix. The tensile moduli of the different solid blend materials are the same as the tensile moduli of the HMS PP (2 GPa) and linear PP (1.95 GPa) are very similar and also the two polymers are completely miscible. As a consequence, the differences in the mechanical properties of the obtained polymeric cellular materials are mainly related to the differences in the cellular structure, open cell content, cell size, and cell AR, among others, as the density is almost the same for all cellular materials and the polymeric matrixes have very similar properties.[27]

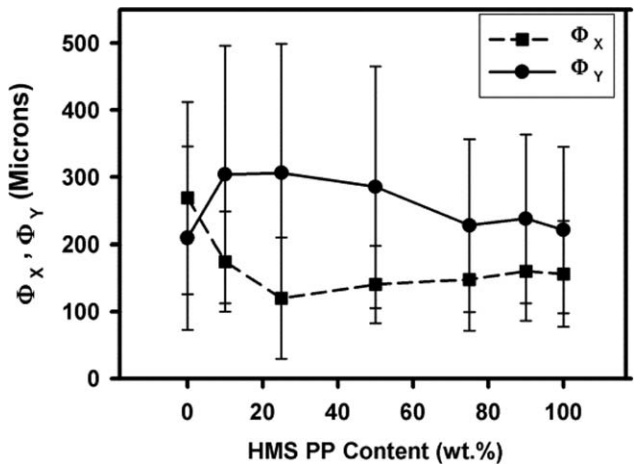

Figure 11. Average chord length in the x and y directions (Φ_x and Φ_y) as a function of the HMS PP content.

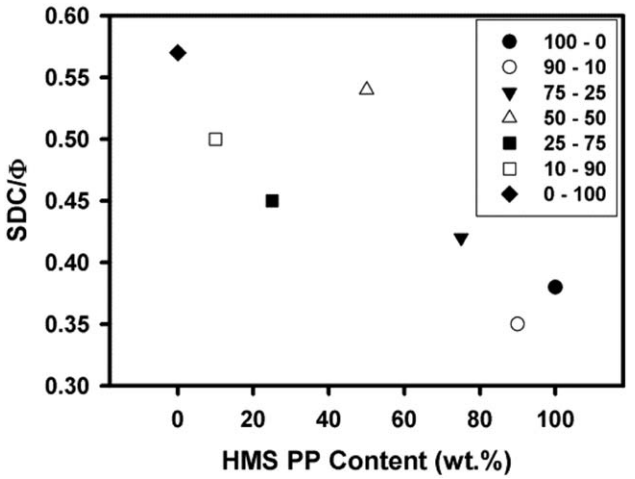

Figure 12. SDC/Φ for the complete collection of PP cellular materials.

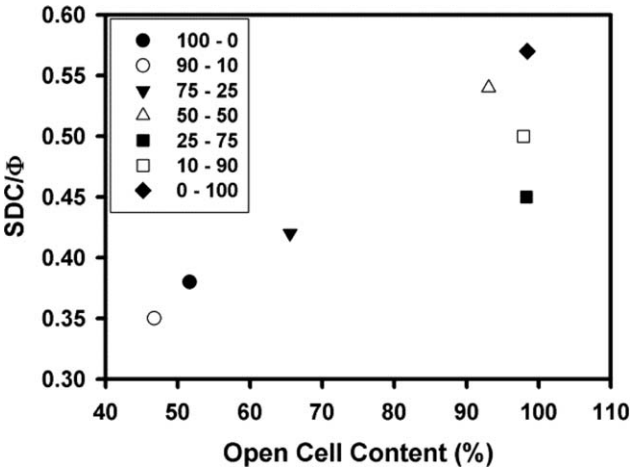

Figure 13. Relationship between SDC/Φ and the open cell content.

Foamed samples were analyzed by performing the compression test aforementioned (in the Experimental section). Experimental

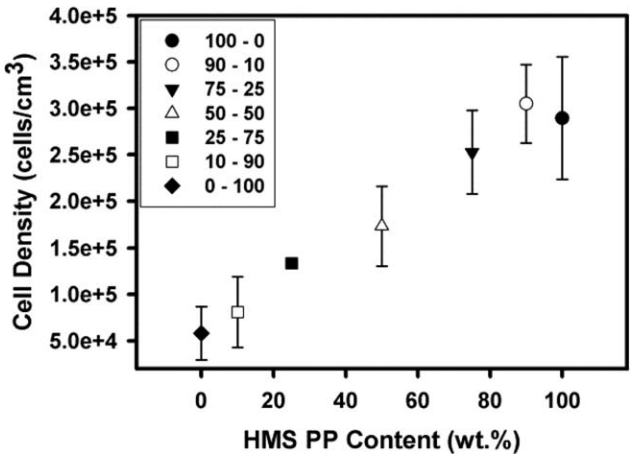

Figure 14. Variation of cell density with the HMS PP content.

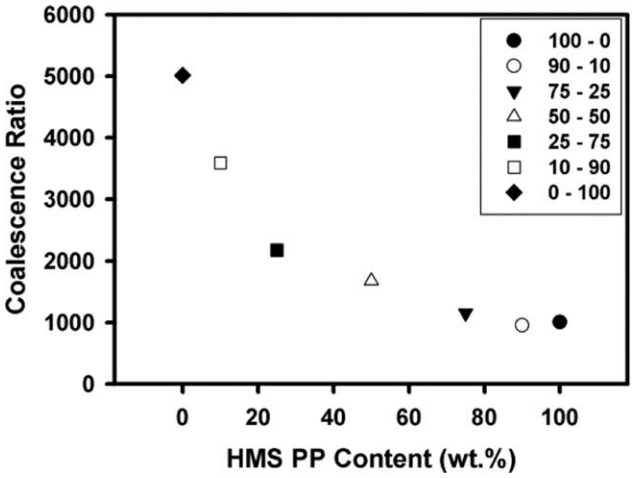

Figure 15. Coalescence ratio as a function of the HMS PP content.

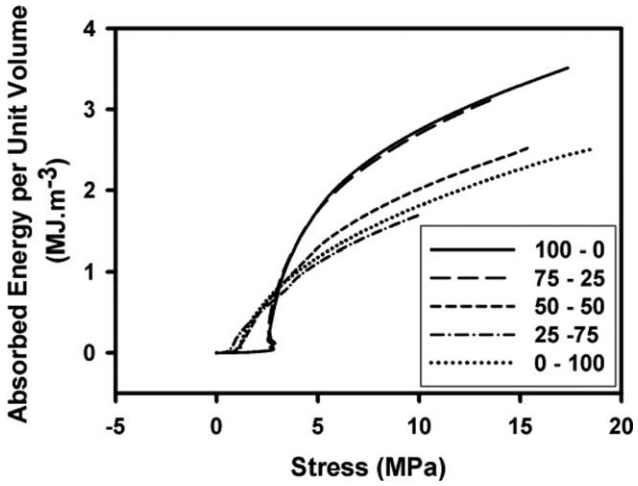

Figure 17. Energy absorption diagrams for samples with different HMS PP content.

results for elastic modulus (E) and collapse stress (σ_C) are summarized in Figure 16 together with the open cell content, to analyze the influence of this parameter on the mechanical behavior.

Comparing the results obtained for the different blends it can be observed that when the amount of HMS PP increases, the stiffness of the foamed blends improves, as the increase in the elastic modulus indicates. The elastic modulus of the cellular materials fabricated with the pure HMS PP is 10 times higher than the elastic modulus of the cellular materials fabricated with the linear PP (even if the density of these last materials is slightly higher). The same behavior is obtained for the collapse stress. There is a significant increase of the collapse stress due to the increase of the HMS PP content. In this case the collapse stress is 2.5 times higher in the cellular materials fabricated with the HMS PP than in those fabricated with the linear PP. The improvement in both mechanical properties is due to a combination of different factors: the reduction of the open cell content, the reduction of the average cell size, and the consequent increase in cell density and the reduction of the standard deviation coefficient of the cell size distribution relative to the cell size, which involves an increase of the homogeneity of the cellular structure. These aspects in turn are related to the extensional behavior of the blends.

The value of absorbed energy per unit volume (W) has also been calculated from the stress–strain curves. Taking into account that cellular materials are typically used as energy absorbers, it is desirable to comprehend how the amount of HMS PP can affect the energy absorption capability. The method used to analyze this characteristic is based on the so-called energy absorption diagrams.[22,27] An energy absorption diagram is obtaining by representing the absorbed energy, W, as a function of the stress. The absorbed energy has been calculated using eq. (11).

$$W = \int_0^{\varepsilon} \sigma(\varepsilon)\ d\varepsilon. \tag{11}$$

Figure 17 shows the absorbed energy per unit volume versus the stress for most of the cellular materials produced.

The best cellular material for a given stress is the one that absorbs the most energy up to this stress.[27] For stresses lower than 2.5 MPa, the cellular materials that contain an amount of HMS PP lower than 50 wt % absorb more energy than materials

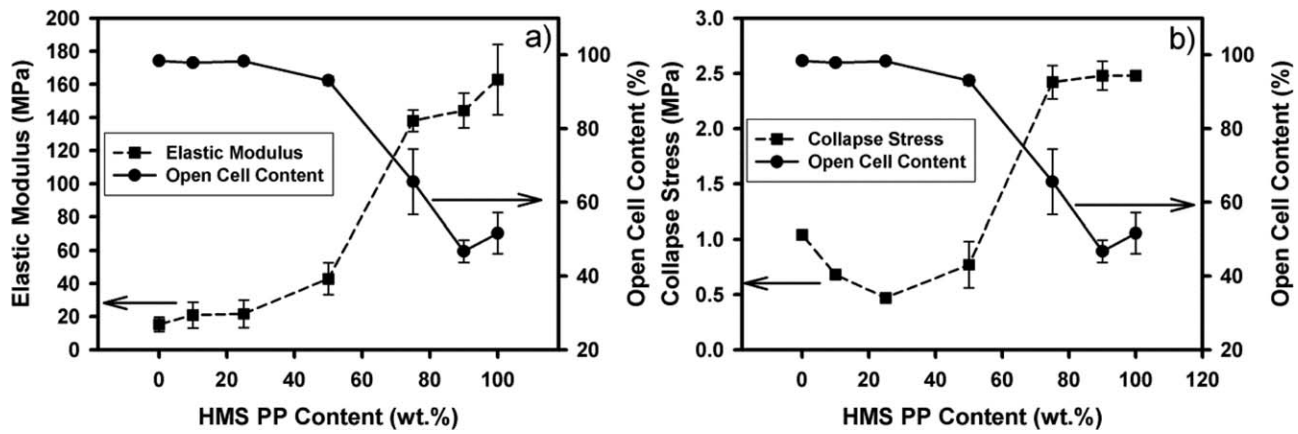

Figure 16. (a) Relationship between the elastic modulus and the open cell content for the different blends. (b) Relationship between the collapse stress and the open cell content for the different blends.

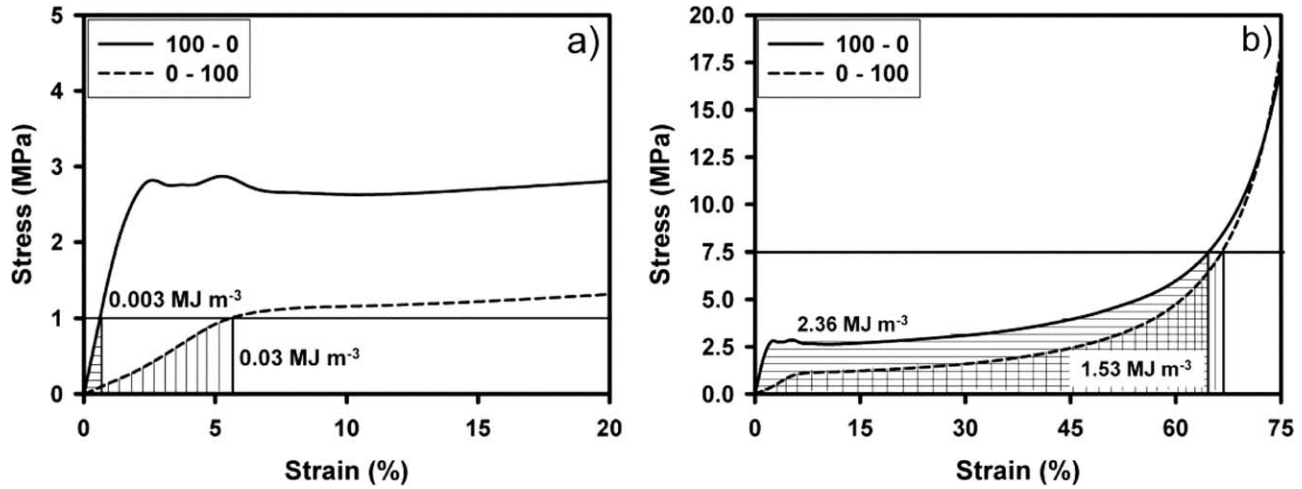

Figure 18. (a) Absorbed energy for a stress of 1 MPa. (b) Absorbed energy for a stress of 7.5 MPa.

that contain an amount of HMS PP higher than 50 wt %. For stresses higher than 2.5 MPa this behavior is completely opposite, the cellular materials that contain the highest amounts of HMS PP are the best energy absorbers. These behaviors are explained graphically in Figure 18 where the stress–strain curves for the materials 100–0 and 0–100 and the correspondent absorbed energy for a stress of 1 and 7.5 MPa are represented.

In the first figure [Figure 18(a)] the absorbed energy (area under the curve) has been calculated for a stress of 1 MPa. As the stiffness of the linear PP is lower than the stiffness of the HMS PP, the energy absorbed by the linear PP is higher than the energy absorbed by the HMS PP. However, for high stress values, the absorbed energy is higher in the HMS PP than in the linear PP as Figure 18(b) shows, indicating that depending on the required properties it is better to use one or the other cellular polymer.

CONCLUSIONS

PP-based cellular materials with very similar density have been fabricated using the ICM route. For this purpose, blends of a HMS PP and a linear PP have been used. The relationships between the extensional rheological properties of the polymeric matrix, the cellular structure, and the mechanical properties of the cellular materials have been analyzed.

The oscillatory shear viscosities satisfy the logarithmic additivity rule, which indicates that the two PPs used are miscible. The shear and extensional rheological properties of the PP blends depend on the amount of the HMS PP in the blend. However, while the extensional properties are highly sensitive to the effect of long-chain branching, the shear viscosity is only slightly decreased by the addition of the HMS PP. Consequently, the differences in the structural and mechanical properties of the resulting PP cellular materials have been related to the changes in the extensional properties.

For cellular materials fabricated with an amount of HMS PP lower than 75 wt % the following results have been obtained. The strain hardening coefficient increases with the amount of HMS PP and consequently the open cell content decreases because the cell walls are able to resist the extension to which they are submitted during the foaming process, without breaking. The cellular structure is also conditioned by the strain hardening coefficient. When the amount of HMS PP increases the cell size decreases and the cell density increases. For high linear PP contents, the cells are completely open and hence the average cell size is larger in these materials. As the cellular materials have the same density if the cell size increases, the cell density decreases. Related to the AR, it was shown that the AR increased with the amount of linear PP. Furthermore, the cell coalescence, in these materials, occurs in a plane perpendicular to the expansion direction and consequently cells are growing considerably in the expansion or thickness direction, making the anisotropy to increase. When the linear PP content is very high the cell anisotropy disappears because the coalescence in these materials is produced in all directions. Moreover, the standard deviation coefficient of the cell size distribution relative to the cell size is higher in the materials containing large amounts of linear PP, indicating that the cellular structure of these materials is more heterogeneous. Finally, the CR has been calculated to analyze the degeneration of the cellular structure during the foaming process. This ratio increases if the linear PP content increases, indicating that the amount of cells that survive during the foaming process is higher in the materials containing large amounts of HMS PP.

Relative to the mechanical properties, as the solid materials have the same properties and the density of cellular materials is the same, the mechanical properties are mainly conditioned by the cellular structure. The elastic modulus and the collapse stress increase with the amount of HMS PP because a homogeneous cellular structure with small cell sizes and also with a considerable content of closed cells leads to good mechanical properties. Moreover, both parameters remain constant for the cellular materials with cells completely open, i.e., for cellular materials fabricated with large amounts of linear PP, indicating that, in this case, the open cell content is the structural parameter which has a larger effect on the mechanical properties. Furthermore, these materials are good energy absorbers provided the stress to which they are subject is less than 2.5 MPa.

On the other hand, cellular materials fabricated with an amount of HMS PP higher than 75 wt % have a completely different

behavior. For these materials the strain hardening coefficient is almost constant and consequently the open cell content, the cell size, the cell anisotropy, the cell density, the CR, the elastic modulus, and collapse stress are also constant and do not change with the amount of HMS PP.

From this study, two main conclusions can be obtained. First, results show that the knowledge of the extensional behavior of the polymeric matrix is fundamental to analyze and understand the cellular structure and the mechanical response of cellular materials. Second, for the relative density analyzed (0.2) the same properties can be obtained with a pure HMS PP and with blends of this PP with a linear PP provided the HMS PP content is higher than 75 wt %.

ACKNOWLEDGMENTS

Financial support from PIRTU contract of E. Laguna-Gutierrez by Junta of Castilla and Leon (EDU/289/2011) and cofinanced by the European Social Fund is gratefully acknowledged. Financial support from the MICINN (MAT 2009-14001 and MAT 2012-34901), the Junta of Castilla and Leon (VA 035U13), and the EU (Nancore Project: EC project number 214148) is gratefully acknowledged.

REFERENCES

1. Frisch, K. C.; Klempner, D. In Handbook of Polymeric Foams and Foam Technology; Klempner, D., Frisch, K. C., Eds.; Hanser Publishers: Munich, Vienna, New York, Barcelona, **1991**; Chapter 1, p 1.
2. Eaves, D. In Handbook of Polymer Foams; Eaves, D., Ed.; Rapra Technology: Shrewsbury, **2004**; Chapter 1, p 1.
3. Rodriguez-Perez, M. A.; Velasco, J. I.; Arencon, D.; Almanza, O.; de Saja, J. A. *J. Appl. Polym. Sci.* **2000**, *75*, 156.
4. Saiz-Arroyo, C.; de Saja, J. A.; Rodriguez-Perez, M. A. *Polym. Eng. Sci.* **2012**, *52*, 751.
5. Saunders, J. H. In Handbook of Polymeric Foams and Foam Technology; Klempner, D., Frisch, K. C., Eds.; Hanser Publishers: Munich, Vienna, New York, Barcelona, **1991**; Chapter 2, p 5.
6. Ibeh, C. C. In Thermoplastic Materials. Properties, Manufacturing Methods and Applications; Ibeh, C. C., Ed.; CRC Press: Boca Raton, **2011**; Chapter 10, p 193.
7. Zheng, W. G.; Lee, Y. H.; Park, C. B. *J. Appl. Polym. Sci.* **2010**, *117*, 2972.
8. Naguib, H. E.; Park, C. B.; Reichelt, N. *J. Appl. Polym. Sci.* **2004**, *91*, 2661.
9. Naguib, H. E.; Park, C. B.; Panzer, U.; Reichelt, N. *Polym. Eng. Sci.* **2002**, *42*, 1481.
10. Lagendijk, R. P.; Hogt, A. H.; Buijtenhuijs, A.; Gotsis, A. D. *Polymer* **2001**, *42*, 10035.
11. Gotsis, A. D.; Zeevenhoven, B. L. F.; Tsenoglou, C. *J. Rheol.* **2004**, *48*, 895.
12. Su, F. H.; Huang, H. X. *J. Appl. Polym. Sci.* **2010**, *116*, 2557.
13. Auhl, D.; Stange, J.; Münstedt, H.; Krause, B.; Voigt, D.; Lederer, A.; Lappan, U.; Lunkwitz, K. *Macromolecules* **2004**, *37*, 9465.
14. Gotsis, A. D.; Zeevenhoven, B. L. F.; Hogt, A. H. *Polym. Eng. Sci.* **2004**, *44*, 973.
15. Park, C. B.; Cheung, L. K. *Polym. Eng. Sci.* **1997**, *37*, 1.
16. Nam, G. J.; Yoo, J. H.; Lee, J. W. *J. Appl. Polym. Sci.* **2005**, *96*, 1793.
17. Reichelt, N.; Stadlbauer, M.; Folland, R.; Park, C. B.; Wang, J. *Cell. Polym.* **2003**, *22*, 315.
18. Spitael, P.; Macosko, C. W. *Polym. Eng. Sci.* **2004**, *44*, 2090.
19. Stange, J.; Münstedt, H. *J. Cell. Plast.* **2006**, *42*, 445.
20. Saiz-Arroyo, C.; de Saja, J. A.; Velasco, J. I.; Rodriguez-Perez, M. A. *J. Mater. Sci.* **2012**, *47*, 5680.
21. Saiz-Arroyo, C.; Rodriguez-Perez, M. A.; Velasco, J. I.; de Saja, J. A. *Composites: Part B* **2013**, *48*, 40.
22. Saiz-Arroyo, C.; Rodriguez-Perez, M. A.; Tirado, J.; Lopez-Gil, A.; de Saja, J. A. *Polym. Int.* **2013**, *62*, 1324.
23. Gibson, L. J. *Mater. Sci. Eng. A* **1989**, *110*, 1.
24. Orwoll, R. A. In Physical Properties of Polymers Handbook, 2nd ed.; Mark, J. E., Ed.; Springer Science: Washington, **2007**; Chapter 37, p 611.
25. Pinto, J.; Solorzano, E.; Rodriguez-Perez, M. A.; de Saja, J. A. *J. Cell. Plast.* **2013**, *49*, 555.
26. Rodriguez-Perez, M. A.; de Saja, J. A. *Cell. Polym.* **1999**, *18*, 1.
27. Almanza, O.; Rodriguez-Perez, M. A.; de Saja, J. A. *Polymer* **2001**, *42*, 7117.
28. Rodriguez-Perez, M. A.; Diez-Gutierrez, S.; de Saja, J. A. *Polym. Eng. Sci.* **1998**, *38*, 831.
29. Gibson, L. J.; Ashby, M. F. In Cellular Solids: Structure and Properties; Gibson, L. J., Ashby, M. F., Eds.; Cambridge University Press: Cambridge, **1997**; Chapter 2, p 15.
30. Gong, W.; Gao, J.; Jiang, M.; He, L.; Yu, J.; Zhu, J. *J. Appl. Polym. Sci.* **2011**, *122*, 2907.
31. Naguib, H. E.; Park, C. B.; Hesse, A.; Panzer, U.; Reichelt, N. In Blowing Agents and Foaming Process Conference 2001. Conference Proceedings, Frankfurt, Germany, March 13–14, 2001, Rapra Technology: Shrewsbury, 2001.
32. Tabatabaei, S. H.; Carreau, P. J.; Ajji, A. *Chem. Eng. Sci.* **2009**, *64*, 4719.
33. Utracki, L. A.; Schlund, B. *Polym. Eng. Sci.* **1987**, *27*, 1512.
34. Wood-Adams, P. M.; Dealy, J. M.; de Groot, A. W.; Redwine, O. D. *Macromolecules* **2000**, *33*, 7489.
35. Liu, C.; Li, C.; Chen, P.; He, J.; Fan, Q. *Polymer* **2004**, *45*, 2803.
36. Gendron, R.; Daigneault, L. E. In Foam extrusion: Principles and Practice; Lee, S. T., Ed.; Technomic Publishing Company: Lancaster, **2000**; Chapter 3, p 35.
37. Stange, J.; Uhl, C.; Münstedt, H. *J. Rheol.* **2005**, *495*, 1059.
38. Chaudhary, A. K.; Jayaraman, K. *Polym. Eng. Sci.* **2011**, *51*, 1749.
39. Rodriguez-Perez, M. A.; Alvarez-Lainez, M.; de Saja, J. A. *J. Appl. Polym. Sci.* **2009**, *114*, 1176.
40. Lee, L. J.; Zeng, C.; Cao, X.; Han, H.; Shen, J.; Xu, G. *Compos. Sci. Technol.* **2005**, *65*, 2344.
41. Lee, S. T.; Park, C. B.; Ramesh, N. S. In Polymeric Foams: Science and Technology; Lee, S. T., Park, C. B., Ramesh, N. S., Eds.; CRC Press: Boca Raton, FL, **2007**; Chapter 5, p 93.